Ab initio calculation of many-body effects on the EEL spectrum of the C(100) surface

Maurizia Palummo,[1] Olivia Pulci,[1] Andrea Marini,[1] Lucia Reining,[2] and Rodolfo Del Sole[1]
[1]*European Theoretical Spectroscopy Facility (ETSF) and Dipartimento di Fisica, Universitá di Roma, "Tor Vergata" Via della Ricerca Scientifica, I-00133 Roma, Italy*
[2]*European Theoretical Spectroscopy Facility (ETSF) and Laboratoire des Solides Irradiés, UMR 7462 CNRS/CEA École Polytechnique, F-91128 Palaiseau, France*
(Received 31 July 2006; revised manuscript received 31 October 2006; published 19 December 2006)

We extend the three-layer model for energy loss calculation to include many-body effects in an *ab initio* framework. The electron energy loss spectrum of the C(100)2×1 surface is calculated and compared with the existing experimental results. We show how many-body effects, namely self-energy, local-fields, and electron-hole interaction, deeply influence the dielectric response and how their inclusion is essential to have good agreement with the experiment. A strong anisotropic behavior of local-field effects on the dielectric response has been observed, while the inclusion of the electron-hole attractive interaction produces a surface-state exciton with binding energy of about 1 eV, confirming a recent theoretical-experimental study of the optical spectra of this surface.

DOI: 10.1103/PhysRevB.74.235431 PACS number(s): 73.61.Cw, 73.61.Ng, 71.35.Cc

I. INTRODUCTION

The importance of excitonic effects on the dielectric response of materials has been known for quite a long time.[1] The appearance of an interacting electron-hole pair during spectroscopical measurements such as light absorption or reflectivity, or electron energy loss, induces a distortion of the spectral line shapes above the gap and the formation of bound exciton states below it.[2] Due to the small screening, this last phenomenon is particularly evident in insulators or in low-dimensional systems, where binding energies of the order of 1 eV are observed.[3,4]

Regarding semiconductor surfaces such as Ge and Si(111) (2×1),[5,6] the optical spectra below 1 eV are currently interpreted in terms of surface-state excitons, with a binding energy of approximately 0.25 eV.[7,8] Stronger excitonic effects are expected on diamond surfaces due to the smaller dielectric constant, and some of us have shown that this is in fact the case for C(100).[9]

The (100) surfaces of homopolar semiconductor compounds are certainly among the most interesting surfaces for their technological applications. Although much effort has been dedicated to Si(100),[10] the high energy gap, the exceedingly high hardness, heat conductivity and hole mobility of diamond and, moreover, the possibility to grow good quality thin films of C(100) by CVD methods, are all motivations for the large number of theoretical and experimental works which have appeared on this surface.[11–13] Both from the theoretical and experimental sides[11–13] it is by now confirmed that the lowest energy configuration for this surface, different from the Si(100), is the 2×1 unbuckled dimers reconstruction. In fact, while the tilting of dimer atoms at Si(100) breaks the surface symmetry and opens the gap, making it semiconducting, the C(100)2×1 with symmetric dimers is already semiconducting and a Jahn-Teller-like transition does not occur. As mentioned in Ref. 14, the different behavior is due to the electronic properties of the constituting atoms: while the C-$2p$ orbital is very well localized, leading to a strong tendency to form a π bond within each dimer, in Si the more extended character of the $3p$ orbital gives rise to more extended bonds, involving neighboring dimers. This is also the origin of the different anisotropy observed in the optical spectra[15,16] and it is one of the main factors which determines the occurrence of a strongly bound exciton only at C(100) and not at Si(100).[17]

Electron energy loss spectroscopy (EELS) is more surface sensitive than optical spectroscopy, because electrons penetrate much less than photons. Recent works[18] have shown its potentiality; by comparing losses with transferred momentum $\mathbf{q}$ along different surface directions, a loss anisotropy spectroscopy technique, similar to reflectance anisotropy spectroscopy (RAS), has been developed. Moreover, being the energy loss more sensitive to surfaces, where the anisotropy occurs, the anisotropy signal is much greater than in the RAS (up to two orders of magnitude at as-grown, well-ordered, surfaces).

The great potentiality of EELS for surface analysis is, however, hampered by the difficulty of developing a suitable theory. This is more complicated than that of surface optical properties, since it requires the knowledge of the full inverse dielectric function of the semi-infinite solid, for many values of transferred momentum ($\mathbf{q}$) and frequencies (ω). Furthermore, since the potential generated by the incident electron is long ranged, particular care must be paid to avoid the contribution of the back surface of the slab and of the repeated slabs. This can be done by integrating the inverse dielectric function $\epsilon^{-1}(z,z',\omega)$ in a finite region including the front surface but excluding the back surface.[19] This of course increases the computational cost since the selection rule of plane waves, $k'_z=k_z$, does not apply in such a case. These are the bottlenecks of the calculation. Hence, so far, calculations for real surfaces have been carried out only within the three-layer local model. This model has been introduced by McIntire and Aspnes[20] to calculate surface effects on reflectance. A surface layer of thickness d (a few atomic planes) has a dielectric constant ϵ_s, different from that of the bulk crystal, ϵ_b. The reflectance is calculated to first order in d/λ (λ being the light wavelength), which is of the order of one hundredth

or smaller. (This first-order expansion leads to simple formulas without decreasing the accuracy.) Later, in Ref. 21, it has been generalized to anisotropic surfaces, by assuming a diagonal but anisotropic dielectric tensor for the surface layer, and to describe EEL experiments. The advantage for EEL calculations is that a local dielectric function can be easily inverted.

This model, which requires the knowledge of the surface and bulk dielectric functions, can in principle include excitonic effects therein, according to the BSE (Bethe-Salpeter equation) approach.[22] However, to the best of our knowledge, no calculations have been carried out so far to consider excitonic effects in surface EELS. The purpose of this paper is to produce a calculation of surface EELS which, although within the approximate three-layer model, accounts for electron-hole interaction effects.

II. THEORETICAL APPROACH

A. The electron energy loss probability function

Within the dipole-scattering theory[23] and the three-layer model,[21] it is possible to calculate EEL spectra. In this approach, valid when the energy and the momentum transferred to the medium are small, the electrons are assumed to be elastically backscattered by the surface barrier, while the loss occurs outside the surface. The electron scattering probability can be factorized in a kinematic factor $A(\mathbf{k},\mathbf{k}')$ and a loss function $\mathrm{Im}[g(\mathbf{q},\omega)]$, which depends on the electronic properties of the medium, as

$$P(\mathbf{k},\mathbf{k}') = A(\mathbf{k},\mathbf{k}')\mathrm{Im}[g(\mathbf{q}_\parallel,\omega)] = \frac{2}{(ea_0\pi)^2}\frac{1}{\cos\phi_i}\frac{k'}{k}\frac{q_\parallel}{(q_\parallel^2+q_\perp^2)^2}\cdot \mathrm{Im}\frac{-1}{1+\epsilon_{eff}(\mathbf{q}_\parallel,\omega)}, \quad (1)$$

where $\mathbf{k}$ and $\mathbf{k}'$ are the wave vectors of the incident and scattered electron respectively; ϕ_i is the angle of incidence, $\hbar\omega$ is the energy transfer, $\mathbf{q}_\perp = k_z - k_z'$ and $\mathbf{q}_\parallel = k_\parallel - k_\parallel'$ are the transferred momenta perpendicular and parallel to the surface, respectively. From the kinematics

$$q_\parallel = \sqrt{2E_0}\sin\theta_i - \sqrt{2(E_0-E)}\sin\theta_f, \quad (2)$$

where E_0 is the energy of the primary electron, E is the lost energy; θ_i and θ_f are the angles of the incident and outcoming electron with respect to the surface normal. Assuming that the scattering plane is the yz plane, the effective dielectric function $\epsilon_{eff}(q_\parallel,\omega)$ comes out to be[21]

$$\epsilon_{eff}(q_\parallel,\omega) = \epsilon_s\frac{\epsilon_s+\epsilon_b+(\epsilon_b-\epsilon_s)e^{(-2q_\parallel d\sqrt{\epsilon_{sy}/\epsilon_{sz}})}}{\epsilon_s+\epsilon_b-(\epsilon_b-\epsilon_s)e^{(-2q_\parallel d\sqrt{\epsilon_{sy}/\epsilon_{sz}})}}, \quad (3)$$

where $\epsilon_s = \sqrt{\epsilon_{sy}\epsilon_{sz}}$.

ϵ_{sy} and ϵ_{sz} are the components of the surface dielectric tensor parallel to the y direction, which lies in the surface plane, and to the z direction, perpendicular to the surface, respectively. $d=3.5$ Å is the thickness of the thin layer which we use to describe the surface within the three-layer model.

Equation (3) has been obtained in Ref. 21 by solving Poisson's equation for the total field within an anisotropic, yet local, three-layer model. The effective dielectric function $\epsilon_{eff}(q_\parallel,\omega)$ is a combination of the surface (ϵ_{sy}, ϵ_{sz}) and bulk dielectric functions (ϵ_b). Here we use a more transparent, although equivalent, formula than in Ref. 21. Equation (3) recovers two well-known limits: for $q_\parallel$ going to 0, ϵ_{eff} tends to ϵ_b. This is because the field of the incident electron, decaying as $\exp(-q_\parallel z)$, penetrates deeply into the bulk, so that the surface layer has a small effect on the loss function. Taking into account first order terms in $q_\parallel d$, we get the first order expansion

$$\epsilon_{eff} \simeq \epsilon_{bulk} + q_\parallel d(\epsilon_{sy} - \epsilon_{bulk}^2/\epsilon_{sz})$$

as in Ref. 21. On the contrary, for very large $q_\parallel$, ϵ_{eff} tends to ϵ_s: EELS, in this case is a probe of the very surface. The values of $q_\parallel d$ relevant to the experimental geometry, considered here,[24] are of the order of one, so that the weights of surface and bulk dielectric functions in ϵ_{eff} are comparable. It is important to note that in Eq. (3) the dielectric functions are the optical ones, calculated in the small q limit and depend only on frequency; the $q_\parallel$ dependence of $\epsilon_{eff}(q_\parallel,\omega)$ originates from the averaging procedure over surface and bulk regions. On the other hand, $q_\parallel$ depends on E according to Eq. (2).

The main structure in Eq. (1), the surface plasmon, occurs when the denominator vanishes (no bulk plasmon is derived within this theory, because of the assumption that electrons do not penetrate the sample.[23]) In the case of a perfect bulk termination, $\epsilon_{eff}=\epsilon_{bulk}$, and the usual surface plasmon dispersion is recovered: $\epsilon_{bulk}(\omega)=-1$.[23] The presence of the surface affects this dispersion, which becomes $\epsilon_{eff}(q_\parallel,\omega)=-1$. In addition to surface plasmons, there are, at lower energies, structures arising from peaks in the imaginary part of ϵ_{eff} which describe electron-hole transitions. These, in particular the electron-hole bound states, are the main concern of this work. We are particularly interested in understanding how these many-body effects appear to affect EEL spectra, as compared to optical spectra.

B. The single-particle Kohn-Sham equations and the inclusion of many-body effects

We calculate the dielectric response of the (100) surface of diamond beyond density functional theory (DFT).[25] In fact, it is well known that DFT is a reliable approach to calculate the ground state electronic properties of many-electron systems, but fails to describe correctly the experiments when physical properties involving excited states are required. The Green's functions formalism represents nowadays the systematic first-principle approach to overcome the failures of DFT (see Refs. 26 and 27 and references therein). Since 1985, Hedin's *GW* method has been successfully used to calculate the quasiparticle band structures of materials, generally leading to good agreement with photoemission and inverse photoemission experiments.[28,29] Moreover, when considering spectroscopic properties where electron-hole excitations are created, it is necessary to go beyond a single quasiparticle picture, and two-particles effects (electron-hole interactions) have also to be included. The Bethe-Salpeter equation for the *e-h* Green's function must hence be solved.

Although the theoretical framework has already been known for more than two decades,[2,30] the very large computational effort needed to solve the BSE has prevented its application to real systems, and its *ab initio* solution has become possible only in the last ten years.[22,31–35] Whereas previous studies have been devoted to the investigation of the excitonic effects on the optical spectra, here we apply the BSE formalism to study the effect of the electron-hole interaction on surface electron energy loss spectra.

A three-step procedure is used to obtain the macroscopic dielectric response of the C(100) surface. First, through a DFT-LDA calculation,[36,37] with the use of norm-conserving pseudopotentials,[38] the geometrical structure of the relaxed ground state configuration of the surface is obtained, solving self-consistently the Kohn-Sham equations.[25] In the second step, one-particle excitation energies are obtained. They are the poles of the one-particle Green function and are determined as solutions of the quasiparticle equations. These are formally similar to the Kohn-Sham equations but a nonhermitian, nonlocal energy dependent self-energy operator Σ (Ref. 39) replaces the exchange-correlation potential. In practical calculations, the self-energy is approximated by the product of the Kohn-Sham Green function G times the screened RPA Coulomb interaction W: $\Sigma = iGW$ (see Ref. 26 and references therein). In the third step, through the solution of the Bethe-Salpeter equation, the coupled electron-hole excitations are included.[40] Detailed discussions about this equation are already present in the literature; [22,27,32,34] here, we just recall that its solution involves the study of the following excitonic Hamiltonian:

$$H_{exc}^{(n_1,n_2),(n_3,n_4)} = (E_{n_2}^{QP} - E_{n_1}^{QP})\delta_{n_1,n_3}\delta_{n_2,n_4} - (f_{n_2} - f_{n_1}) \int d\mathbf{r}_1 d\mathbf{r}_1' d\mathbf{r}_2 d\mathbf{r}_2' \phi_{n_1}(\mathbf{r}_1) \times \phi_{n_2}^*(\mathbf{r}_1') \Xi(\mathbf{r}_1, \mathbf{r}_1', \mathbf{r}_2, \mathbf{r}_2') \phi_{n_3}^*(\mathbf{r}_2) \phi_{n_4}(\mathbf{r}_2'),$$

where f_{n_i} are the occupation numbers, $E_{n_i}^{QP}$ are the quasiparticle (GW) eigenvalues, and ϕ_{n_i} are the Kohn-Sham one-particle wave functions.[41] The kernel Ξ contains two contributions: W, which is the attractive screened Coulomb electron-hole interaction and $\bar{v}$, which is the bare Coulomb interaction where the long range term with vanishing wave vector is eliminated; $\bar{v}$ describes local field effects in a way equivalent to the Adler-Wiser approach when the electron-hole attraction W is neglected.[27,42] We use $\bar{v}$, rather than the full Coulomb potential v, which is appropriate for energy loss calculations, because Eq. (3) involves the optical (macroscopic) dielectric functions. This is expected to be correct for small momentum transfer.

C. Computational details

We model the C(100)2×1 surface by a repeated slab containing 12 atomic C layers and a vacuum region equivalent to 8 atomic layers. A norm-conserving pseudopotential generated within the Martins-Trouiller scheme is used.[38] Careful convergence tests on bulk diamond allow us to use a kinetic energy cutoff of 40 Ry and give an equilibrium lattice parameter, a_0, and bulk modulus, B_0, of 6.73 a.u. and 4.5 Mbar (experimental values are 6.74 and 4.42, respectively). The stable surface geometry agrees well with previous results:[14,43] it consists of symmetric dimers with a bond length of 1.37 Å. We used 16 $\vec{k}$ points in the full BZ for self-consistency and 128 k points for the optical properties. The convergence of the dielectric function increasing the number of k points to 256 in the BZ has been tested at the RPA level. We also checked the convergence of the optical spectra with respect to the number of atomic and vacuum layers. Regarding the GW part of the calculation, we computed the matrix elements of $\epsilon^{-1}(G,G',q,\omega)$ within a plasmon-pole model, using 1367 plane waves and 13 $\mathbf{q}$ vectors within the two-dimensional irreducible part of the Brillouin zone (IBZ). The correlation part of the self-energy Σ_c has been calculated using 1367 planewaves and 1000 bands, while 3157 planewaves have been necessary for the exchange part Σ_x. For the solution of the Bethe-Salpeter equation, we used the Haydock recursion method[33,44] which allows us to treat large excitonic matrices. We verified that 30 valence bands and 40 conduction bands describe correctly the dielectric function in the energetic region between 0 and 18 eV. Adding a reasonable high energy tail does not change the energy positions of the energy loss peaks in the range up to 7 eV, which are those of interest in the present paper.

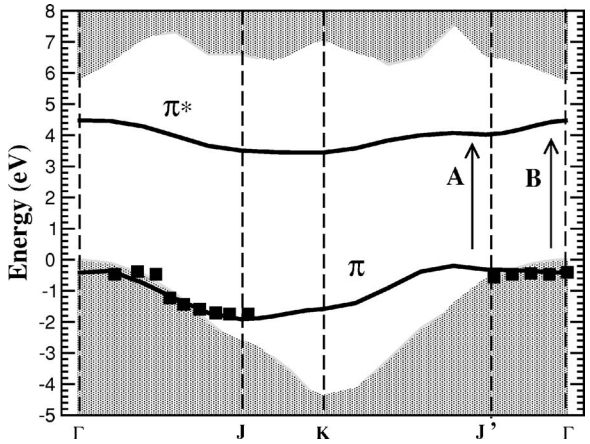

FIG. 1. Electronic band structure of (100) surface along high-symmetry lines of the 2×1 BZ including GW corrections. Grey regions indicate the projected bulk band structure; solid lines are the π and π^* dimers surface states. Experimental data from Ref. 45.

III. RESULTS AND DISCUSSION

Our results for the electronic band structure, obtained including the GW corrections, are shown in Fig. 1 together with direct photoemission data by Graupner *et al.*[45] The agreement between theory and experiment is very good. In Table I we list the surface electronic gaps at high-symmetry points of the IBZ. The QP corrections open the LDA gaps between occupied and empty surface states by 1.8–2.1 eV. The GW corrections do not much affect the dispersion of the states, leaving the minimum surface gap indirect (from around J' to K) and the surface bands almost parallel near J' (see Fig. 1). This parallelism, together with the low dielectric

TABLE I. DFT-LDA gaps between surface states at some high-symmetry k points are compared with the *GW* corrected values. Also the electron affinity χ, defined as $\chi=E_{vacuum}-E_{BCB}$, with E_{BCB} energy of the bottom of the conduction band, is shown in the last column. All energies are in eV.

	$\bar{\Gamma}$	$\bar{J}$	$\bar{K}$	$\bar{J}'$	χ
DFT-LDA	2.7	3.2	2.9	2.2	1.9
GW	4.8	5.3	5.0	4.0	1.1
Exp.					0.5[a], 0.75[b], 1.3[c]

[a]Reference 11.
[b]Reference 47.
[c]Reference 48.

screening of diamond, is the main reason for the formation of a strongly bound exciton. Kress *et al.*[46] obtained, using a simplified *GW* scheme for the screening, similar results but a slightly larger opening of the surface state gaps (2.14–2.35 eV).

In Table I we also show our calculated electron affinity χ, that in DFT takes the value of 1.9 eV, out of the experimental range [from 0.5 to 1.3 eV (Refs. 11, 47, and 48)]. The inclusion of QP effects, instead, allows for a better agreement with the measurements, since our *GW* value for χ, 1.1 eV, falls well within the experimental range.

The imaginary part of the surface dielectric function, defined as the dielectric response of the first few surface atomic layers, is shown in Fig. 2.[49] Two light polarizations have been considered, along the dimers (full lines) and perpendicular to the dimers (dashed lines). Different levels of approximation in the theoretical approach are shown in the three panels, from DFT to *GW* to BSE. In the top panel (DFT-LDA level) we see that two peaks (*A* and *B*), at 2.4 and 3 eV, which are due to surface-state to surface-state transitions, are present only for light polarized along the dimers (full lines), while for light polarized perpendicular to the dimers (dashed lines) the absorption onset occurs at 3.8 eV. This result reproduces the strong anisotropy of the macroscopic dielectric functions predicted in other theoretical papers.[15,16] On the central panel (self-energy effects included) we observe that the *GW* dielectric functions are essentially blue shifted by about 1.9 eV with respect to the DFT curves. Finally, on the third panel, when the *e-h* attractive interaction (W) and the local field effects ($\bar{v}$) are included through the solution of the Bethe-Salpeter equation, the surface dielectric function is redshifted by about 1 eV and a significative shape and intensity modification is observed. The two peaks appearing at about 3.1 and 3.8 eV in Fig. 2(c) are due to bound exciton states, occurring below the relative surface QP gaps, respectively near J' and Γ. By analyzing the energetic positions of the lowest eigenvalues of the excitonic Hamiltonian, we know that the lowest-energy exciton is located at 3.1 eV, hence we can estimate an excitonic binding energy of 0.9 eV. To better analyze this result, we show in Fig. 3 the effect of $\bar{v}$ (that is, of the local fields effects) and of W (that is the attractive *e-h* interaction) separately, on the surface dielectric function. From the *GW*+LF curves (diamonds) we can immediately note the anisotropic role of local fields on the surface low energy peak. In fact, while for light polarization parallel to the dimers, the LFs produce a strong reduction of the *GW* peaks (full line, lower panel), for the perpendicular polarization their influence is even not visible in the figure (upper panel). This behavior can be understood keeping in mind the atomic geometry of the surface reconstruction: along the [011] direction, parallel to the dimers (and perpendicular to the dimers rows), wide vacuum regions between the surface atoms are present. In the [0–11] direction (which is the direction of the dimers rows) the atomic distances are similar to the bulk ones. In other words, the electric field for light polarized along [011] undergoes a surface distortion, such as to keep, according to Maxwell's boundary conditions, its electric displacement constant within the dimer rows and in between. This induces a strong reduction of the electric field within the dimer rows, and hence of the dielectric response for light polarized along the dimers ([011] direction). A similar anisotropic behavior of local-field effects (the so-called "depolarization effect") has been observed in other strong anisotropic systems such as nanowires and nanotubes.[50]

Moreover, we see from Fig. 3 that also the screened electron-hole Coulomb interaction (W) in the BS kernel has an anisotropic effect (dashed lines). In fact, it induces a red

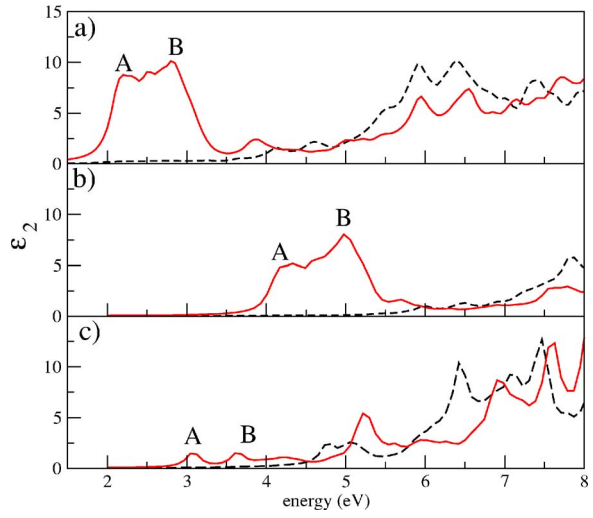

FIG. 2. (Color online) Imaginary part of the surface dielectric functions of C(100) 2×1 surface for light polarized along the dimers (full lines) and in the perpendicular direction (dashed line). (a) RPA curves at DFT-LDA level. (b) *GW* effects included. (c) Self-energy (*GW*), local-field (LF), and excitonic (Exc) effects included. An artificial broadening of 0.1 eV has been used.

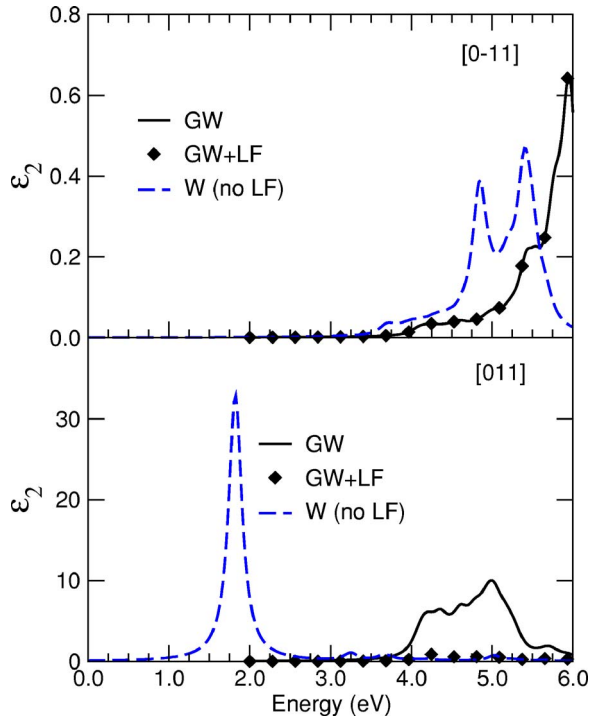

FIG. 3. (Color online) Upper panel: Imaginary part of the surface dielectric functions for light polarized along the dimer rows. Solid line: *GW* calculation; diamonds: effect of the local fields $\bar{v}$ (*GW*+LF calculation); dashed line: effect of W (no LF included in the BSE kernel). Lower panel: as before but for light polarized along the dimers.

shift of different entity for the two light polarizations, because the excitonic effect is much larger for light polarized along the dimers, as in isolated molecules. The interplay of LF and electron-hole attractive interaction (W) leads to the curve shown in the lower panel of Fig. 2 with the excitonic peaks (A and B) still occuring for light polarized along the dimers, although with intensities strongly reduced by the local-field effects. The RAS calculated with these ingredients is in good agreement with the experiments.[9]

In Fig. 4 the theoretical EEL spectra, obtained including *GW* corrections [panel (c)], *GW*+LF [panel (d)] and *GW* +LF+Exc effects [panel (b)] are compared with the experiments of Ref. 24 [panel (a)]. The experiment was performed with a primary beam energy of 50 eV and at a fixed angle of incidence $\phi_i=60°$ under specular reflection. Thanks to the high energetic primary beam and to the small energy loss, the use of dipole-scattering theory is allowed and the comparison of our theoretical results with the experimental curve is justified. The dependence of $q_\parallel$ on E, according to Eq. (2) is included in the calculation. A typical value of the transferred momentum in this experimental configuration is $q_\parallel \simeq 0.15$ a.u.

The experimental loss function is characterized by three main peaks located at 3.5, 4.7, and 5.9 eV. We can see that the agreement of the theoretical results with the experiment is reasonably good *only when* self-energy, local-field, and excitonic effects are included altogether [panel (b)]. In fact, while the *GW* curve [panel (c)] has an onset at about 4 eV and the effect of LF is essentially a reduction of its intensity

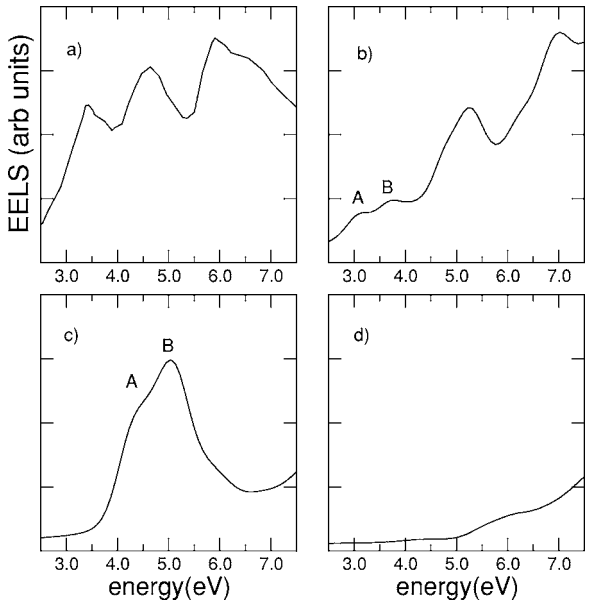

FIG. 4. Electron energy loss spectrum of C(100) 2×1 surface. Panel (a) Experimental spectrum from Ref. 24. Panel (b) Theoretical spectrum with self-energy, local field, and excitonic effects included (*GW*+LF+Exc). Panel (c) As before but with only self-energy effects included (*GW*). Panel (d) As before but with self-energy and local field effects included (*GW*+LF).

[panel (d)], only the *GW*+LF+Exc spectrum reproduces the three main experimental peaks. The lowest energy double peak (centered around 3.5 eV) is due to the excitation of the surface-state excitons, appearing at 3.1 and 3.8 eV in the surface dielectric functions; the calculated double peak corresponds well to the asymmetric experimental structure around 3.4 eV. The calculated structure at about 5 eV is due to surface state–surface state transitions, and the higher structures are mixed surface state–bulk state transitions. These interpretations are clarified looking at the imaginary and real parts of $\epsilon_{eff}(q_\parallel,\omega)$ which are reported in Fig. 5 (left and right panels, respectively), where $q_\parallel$ again depends on E, according to Eq. (2). All the loss structures mentioned so far originate from the imaginary part of ϵ_{eff}, as shown by the

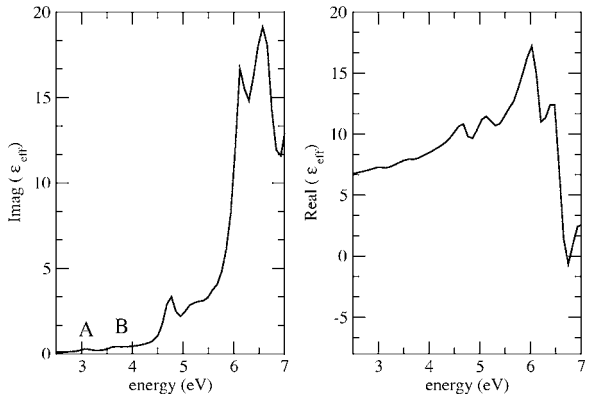

FIG. 5. Imaginary (left panel) and real (right panel) parts of theoretical (*GW*+LF+Exc) effective dielectric function $\epsilon_{eff}(q_\parallel,\omega)$, with $q_\parallel$ calculated according to Eq. (2).

corresponding labels in Figs. 4(b) and 5 (left panel). Finally, the calculated loss structure close to 6.7 eV has also a contribution from the dip in the real part of ϵ_{eff} occurring at the same energy, which makes the denominator of Eq.(1) very small (it would vanish for $\epsilon_{eff}=-1$, when a surface plasmon occurs).

IV. CONCLUSIONS

In the present paper, we have investigated how the electron-hole interaction affects the EELS, and described in detail how to include many-body effects in the three-layer model within a dipole scattering approximation. In a combined theoretical-experimental study of the reflectance anisotropy spectrum of the C(100) surface,[9] it has been recently shown that strongly bound surface-state excitons, with binding energy of approximately 1 eV, exist at this surface. From a comparison of the theoretical EELS spectrum with the existing experiment,[24] we confirm the existence of strongly bound surface-state excitons at the C(100)2×1 surface. EEL line shapes are of course different from optical ones, nevertheless the presence of strongly bound excitons is clearly revealed. The theoretical EEL spectrum is in good agreement with the measured one *only when* all many-body effects (namely, self-energy, local-field and excitonic effects) are considered all together.

ACKNOWLEDGMENTS

This work was funded in part by the EU's Sixth Framework Programme through the Nanoquanta Network of Excellence (NMP4-CT-2004-500198), and by MIUR through NANOSIM and PRIN 2005. We acknowledge the CINECA CPU time granted by INFM. Useful discussions with Valerio Olevano are gratefully acknowledged.

[1] F. Bassani and G. Pastori Parravicini, *Electronic States and Optical Transitions in Solids*, edited by R. A. Ballinger (Pergamons, New York, 1975).
[2] W. Hanke, Adv. Phys. **27**, 287 (1978).
[3] L. X. Benedict, E. L. Shirley, and R. B. Bohn, Phys. Rev. Lett. **80**, 4514 (1998).
[4] A. Ruini, M. J. Caldas, G. Bussi, and E. Molinari, Phys. Rev. Lett. **88**, 206403 (2002).
[5] G. Chiarotti *et al.*, Phys. Rev. Lett. **21**, 1170 (1968).
[6] P. Chiaradia, A. Cricenti, S. Selci, and G. Chiarotti, Phys. Rev. Lett. **52**, 1145 (1984).
[7] L. Reining and R. Del Sole, Phys. Rev. Lett. **67**, 3816 (1991); M. Rohlfing and S. G. Louie, *ibid.* **83**, 856 (1999).
[8] M. Rohlfing, M. Palummo, G. Onida, and R. Del Sole, Phys. Rev. Lett. **85**, 5440 (2000).
[9] M. Palummo, O. Pulci, R. Del Sole, A. Marini, M. Schwitters, S. R. Haines, K. H. Williams, D. S. Martin, P. Weightman, and J. E. Butler, Phys. Rev. Lett. **94**, 087404 (2005).
[10] T. Yokoyama and K. Takayanagi, Phys. Rev. B **61**, R5078 (2000); M. Ono, A. Kamoshida, N. Matsuura, E. Ishikawa, T. Eguchi, and Y. Hasegawa, *ibid.* **67**, 201306 (2003); H. Okada, Y. Fujimoto, K. Endo, K. Hirose, and Y. Mori, *ibid.* **63**, 195324 (2001).
[11] F. Maier, J. Ristein, and L. Ley, Phys. Rev. B **64**, 165411 (2001).
[12] M. D. Winn, M. Rassinger, and J. Hafner, Phys. Rev. B **55**, 5364 (1997); Z. Zhang, M. Wensell, and J. Bernholc, *ibid.* **51**, 5291 (1995).
[13] J. Ristein, Appl. Phys. A **82**, 377 (2006); S. J. Sque, R. Jones, and P. R. Briddon, Phys. Rev. B **73**, 085313 (2006).
[14] P. Kruger and J. Pollmann, Phys. Rev. Lett. **74**, 1155 (1995).
[15] C. Kress, A. I. Shkrebtii, and R. Del Sole, Surf. Sci. **377**—379, 398 (1997).
[16] V. I. Gavrilenko and F. Bechstedt, Phys. Rev. B **56**, 3903 (1997).
[17] Similar calculations have been carried out [M. Palummo, A. Marini, O. Pulci, and R. Del Sole (unpublished)] for the Si(100) surface, where a small redshift of the surface states peak is observed, compatible with the formation of a bound exciton with binding energy of about 100 meV.
[18] A. Balzarotti, M. Fanfoni, F. Patella, F. Arciprete, E. Placidi, G. Onida, and R. Del Sole, Surf. Sci. **524**, 71 (2003); E. Placidi, C. Hogan, F. Arciprete, M. Fanfoni, F. Patella, R. Del Sole, and A. Balzarotti, Phys. Rev. B **73**, 205345 (2006).
[19] C. Hogan and R. Del Sole (private communication).
[20] J. D. E. McInthire and D. E. Aspnes, Surf. Sci. **24**, 417 (1971).
[21] A. Selloni and R. Del Sole, Surf. Sci. **168**, 35 (1986).
[22] S. Albrecht, L. Reining, R. Del Sole, and G. Onida, Phys. Rev. Lett. **80**, 4510 (1998).
[23] H. Ibach and D. L. Mills, *Electron Energy Loss Spectroscopy and Surface Vibrations* (Academic, New York, 1982).
[24] T. W. Mercer and P. E. Pehrsson, Surf. Sci. **L327-L331**, 399 (1998).
[25] P. Hohenberg and W. Kohn, Phys. Rev. **136**, B864 (1964). W. Kohn and L. J. Sham, *ibid.* **140**, A1113 (1965).
[26] F. Aryasetiawan and O. Gunnarsson, Rep. Prog. Phys. **61**, 237 (1998).
[27] G. Onida, L. Reining, and A. Rubio, Rev. Mod. Phys. **74**, 601 (2002).
[28] Mark S. Hybertsen and Steven G. Louie, Phys. Rev. B **32**, 7005 (1985).
[29] R. W. Godby, M. Schlüter, and L. J. Sham, Phys. Rev. B **37**, 10159 (1988).
[30] G. Strinati, Riv. Nuovo Cimento **11**, 1 (1988).
[31] G. Onida, L. Reining, R. W. Godby, R. Del Sole, and W. Andreoni, Phys. Rev. Lett. **75**, 818 (1995).
[32] M. Rohlfing and S. G. Louie, Phys. Rev. Lett. **80**, 3320 (1998).
[33] L. X. Benedict and E. L. Shirley, Phys. Rev. B **59**, 5441 (1999).
[34] L. X. Benedict, E. L. Shirley, and R. B. Bohn, Phys. Rev. Lett. **80**, 4514 (1998).
[35] P. H. Hahn, W. G. Schmidt, and F. Bechstedt, Phys. Rev. Lett. **88**, 016402 (2002).
[36] D. M. Ceperley and B. J. Alder, Phys. Rev. Lett. **45**, 566 (1980); J. P. Perdew and A. Zunger, Phys. Rev. B **23**, 5048 (1981).
[37] First-principles computation of material properties: the ABINIT software project (URL http://www.abinit.org); X. Gonze J.-M. Beuken, R. Caracas, F. Detraux, M. Fuchs, G.-M. Rignanese, L.

Sindic, M. Verstraete, G. Zerah, F. Jollet, M. Torrent, A. Roy, M. Mikami, Ph. Ghosez, J.-Y. Raty, D. C. Allan, Comput. Mater. Sci. **25**, 478 (2002).

[38] N. Troullier and J. L. Martins, Phys. Rev. B **43**, 1993 (1991).

[39] L. Hedin, Phys. Rev. **139**, A796 (1965).

[40] The many-body effects have been included using tools developed within the network of Excellence "Nanoquanta" (http://www.cmt.york.ac.uk/nanoquanta/). The BSE calculations were performed with the codes EXC (http://theory.polytechnique.fr/codes/exc/), and SELF (http://www.fisica.uniroma2.it/~self/).

[41] The excitonic Hamiltonian contains a part with positive excitation energies (n_2 empty and n_1 filled), which yields a polarization term resonant for positive energies (the so-called resonant part), another part with negative excitation energies (n_2 filled and n_1 empty), which yields a polarization resonant at negative energies (the so-called antiresonant part). We neglect here the coupling part of the excitonic Hamiltonian. Recently (V. Olevano, L. Reining, Phys. Rev. Lett. **86,** 5962 (2001)), it has been shown that the coupling part may have important effects on the plasmons, which occur anyway at energies higher than those considered here.

[42] S. L. Adler, Phys. Rev. **126**, 413 (1962); N. Wiser, *ibid.* **129**, 62 (1963).

[43] J. Furthmuller, J. Hafner, and G. Kresse, Phys. Rev. B **55**, 7334 (1997).

[44] R. Haydock, Comput. Phys. Commun. **20**, 11 (1980).

[45] R. Graupner, F. Maier, J. Ristein, L. Ley, and C. Jung, Phys. Rev. B **57**, 12397 (1998).

[46] C. Kress, M. Fiedler, W. G. Schmidt, and F. Bechstedt, Phys. Rev. B **50**, 17697 (1994).

[47] P. K. Baumann and R. J. Nemanich, Surf. Sci. **409**, 329 (1998).

[48] L. Diederich, O. M. Küttel, P. Aebi, and L. Schlapbach, Surf. Sci. **481**, 219 (1998).

[49] From the repeated slab (RS) dielectric responses (which are the outputs of the *ab initio* calculations) we extract the single-slab (SS) dielectric responses as (Ref. 24) $\epsilon_{\parallel}^{SS}(\omega)=\epsilon_{\parallel}^{RS}\frac{(d_v+d_s)}{d_s}-\frac{d_v}{d_s}$, and $\frac{1}{\epsilon_{\perp}^{SS}(\omega)}=\frac{1}{\epsilon_{\parallel}^{RS}}\frac{(d_v+d_s)}{d_s}-\frac{d_v}{d_s}$, where $d_v=10.8$ Å, and $d_s=16.2$, are the vacuum and atomic layers thickness, respectively. The surface dielectric functions are obtained subtracting from these quantities, the bulk contribution. This is done considering a thickness of the surface layer equal to $d=3.5$ Å.

[50] A. G. Marinopoulos, Lucia Reining, Angel Rubio, and Nathalie Vast, Phys. Rev. Lett. **91**, 046402 (2003).